

Slag emulsification in the continuous casting process

Piotr R. Scheller, Rene Hagemann

Freiberg University of Mining and Technology, Institute of Iron and Steel Technology

34 Leipzigerstrasse 34, 09596 Freiberg, Germany

Abstract: In the continuous casting the mould flux on the meniscus of liquid steel can be introduced into the liquid steel producing defects on final product. Conditions leading to the instabilities near the slag/steel interface were investigated. Two main parameters promote the emulsification process: convective flow in the liquid metal and the interfacial convection caused by mass exchange between both phases.

In the first part of present work, the stability of a liquid-liquid interface without mass transfer between phases was investigated in cold model study using a single - roller driven flow in oil - water systems with various oil properties. Using the similarity theory, two dimensionless number were identified, *viz.* capillary number Ca and the material number Λ , which are suitable to describe the force balance for the problem treated. The critical values of the dimensionless capillary number Ca for droplet break-up marking the start of their entrainment into the lower fluid are determined over a wide-range of fluid properties. Another dimensionless number Λ was defined as the ratio of kinematic viscosities of the dispersed phase ν_d and continuous phase ν_c , (*viz.* kinematic viscosity ratio). The material numbers of different steel - slag systems were calculated using measured thermo - physical properties. With the knowledge of thermo - physical properties of steel - slag systems, the critical capillary number Ca^* for slag entrainment as a function of Λ could be derived. Assuming no reaction between the phases and no interfacial flow, slag entrainment should not occur under usual casting conditions.

In the second part of the present work, the effect of the interfacial convection on the emulsification process was investigated. The interfacial convection is caused by the local change of the interfacial energy. Based on the investigation of the mass exchange in the industrial process the relationship between mass exchange and interfacial convection were derived using dimension free description. Additionally the model experiments with direct observation of the interfacial convection in the Confocal Laser Scanning Microscope were performed and the slag emulsification detected.

Keywords: continuous casting, slag emulsification, interface stability, interfacial energy, mass transport

1. Introduction

In steelmaking processes the emulsification of steel in slag and vice versa takes place. The resulting increase of interfacial area between both phases leads to higher reaction rates. In the last stage of liquid steel processing, in the continuous casting process, the emulsification should be prevented as slag particles cause defects in rolled products and steel particle in liquid flux affect their solidification^[1]. The energy supply is necessary to emulsify the immiscible fluids in each other. In metallurgical processes this energy is supplied usually in the form of flow energy as bulk flow near the

interface and/or as the interfacial convection. In continuous casting process, the interface between steel and slag should be stable to avoid the break-up of slag droplets forming non-metallic inclusions, which deteriorate the product quality [2]. In the present paper, the term entrainment is used to describe the break-up of slag droplets from the steel - slag interface by shear stress. Thomas investigated slag entrainment caused by vortex formation due to asymmetrical mould flow using numerical simulation [3]. To get an insight into the mechanism of slag entrainment, model liquids were used to predict the behavior of the steel - slag interface under shear stress conditions [4][5] when generating the flow near the interface. Savolainen *et al.* [4] studied the influence of the thermo - physical properties in systems of two immiscible fluids. They pointed out that an increase of the three parameters, *viz.* oil viscosity, density difference and interfacial tension, results in an increase of critical fluid flow velocity for slag entrainment. The break-up of droplets of one fluid suspended in a second fluid with density ratio (density of the continuous phase divided by the density of the dispersed phase) $\rho_c/\rho_d = 1$ induced by velocity lag between the continuous phase and the dispersed droplets was studied extensively in a coquette - device and four - roller apparatus at low temperatures. The break-up of droplets in a steady shear flow depends on the viscosity ratio η_d/η_c (viscosity of the dispersed phase divided by the viscosity of the continuous phase) and on critical capillary number Ca^* [6][7]. The capillary number as a function of the viscosity ratio describes therefore a stability criterion between stable and unstable droplets. Increasing the capillary number to its critical value Ca^* results in droplet break-up producing two or more smaller droplets [8][9]. Figure 1 illustrates the situation in the continuous casting mould. Shear stresses are generated between the steel flow and the liquid flux layer. At the steel - slag interface, two convection flows lead to slag entrainment: A macroscopic shear flow and an interfacial flow (Marangoni flow), which is generated by a local difference of the interfacial tension caused e.g. by chemical reactions.

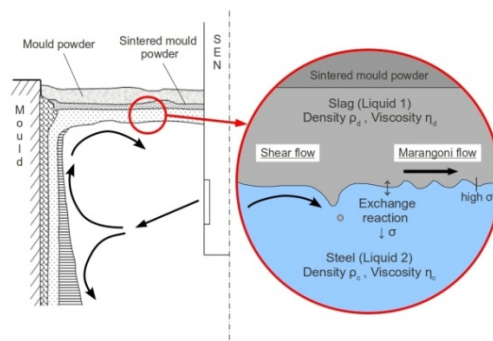


Figure 1 Possible flow conditions and slag entrainment at the steel - slag interface in continuous casting mould.

Another aspect are the reactions at the interface producing lower interfacial energy and their gradients. In e.g. the continuous casting the thin liquid flux layer at the meniscus reacts with liquid steel before it infiltrate the gap between the steel shell and the mould wall. Some aspects of transport phenomena for the case of thin slag layer reacting with liquid steel will be analysed in this paper and the experimental results presented.

Convection flow in the fluid phases have a decisive effect on mass and heat transport. In the case of reactions between the metal and the slag, the flows and the mixing in the slag phase determine the kinetics of the reactions because of higher viscosity [10]. Here a distinction can be drawn between large area, thermal convective flows taking

place under specific conditions, and convective flows in the vicinity of the interface occurring, for example, finally as a result of chemical reactions at the phase boundary ^[11].

Gradients of interfacial energy along the interface produces interfacial convection which increases the mass transport within and through the boundary layers. These gradients can be generated by e.g. the gradients of temperature, concentration, electrical potential which in turn are usually caused by local differences of species transfer through the interface and their diffusion. In slag-metal systems such convection reaches high intensity ^{[12][13][14]} because of high values of interfacial energies. In the most of systems the interfacial energy decreases with increasing mass flow rate through the interface of diffusing components. The instability of the interface between two undisturbed and still fluids is therefore dependent on the quote of the diffusion coefficients in both phases of the passing through component and on the quote of the kinematical viscosities of both phases. Therefore the fluid dynamic controlled instability occurs if e.g. is $D_1/D_2 = 1$ and $\nu_1/\nu_2 > 1$ ^[15]. These conditions are still fulfilled for liquid slag/metal systems ^[16]. The induced flow generates in this case microwaves at the interface which is termed the Kelvin-Helmholtz instability and was reported in few papers ^{[17][18][19]}.

2. Experimental

2.1 Experimental set-up

Figure 2a) shows the schematic drawing of the experimental apparatus consisting of a reservoir with roller, driving motor and measuring unit. The rectangular water reservoir with the dimensions $0.2 \times 0.08 \times 0.08 \text{ m}^3$ was made of acrylic material. Inside the container a plastic roller with a diameter of 40 mm and a length of 60 mm was mounted. The roller was linked to a d.c. motor with controlled rotating speed. Figure 2b) shows schematically the arrangement for the entrainment study of upper liquid in the lower liquid. For the liquid - liquid study, the roller was located 10 mm below the interface in the reservoir and the oil layer thickness was 10 mm which was carefully stratified. The oil layer was dyed by oil soluble colour for better visualisation of the entrainment process. A high speed camera in front of the acrylic vessel recorded the process of meniscus formation and droplet break-up with 300 frames per second.

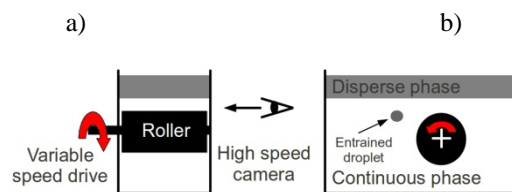


Figure 2 Front view: Configuration of the experimental setup consisting of drive, roller and high speed camera; b) Side view: liquid level for experiment of upper liquid entrainment.

For analysing the experiments, the open source software Avidemux ^[20] was used. With the help of a mark on the roller and the frame number, it was possible to calculate the rotation speed and the critical rotation rate $n_{crit.}$ for the first entrained droplet. For each experimental run with other oil – water system, both liquids were renewed. At the start of the experiment, the roller rotated with a low rotation speed which was slowly increased by the motor. During the acceleration of the roller, the velocity gradient between roller and the interface would increase and the interface would

be exposed to an increasing velocity gradient. Reaching a critical rotation number n_{crit} , droplet break-up appears (compare Figure 2b). With the observation of the first entrained droplet, the experimental run ends and after a rest time, initial conditions for the interface are adjusted and the next was run started. For the observation of the interfacial convection the rectangular container with the dimensions of $0.21 \times 0.07 \times 0.05 \text{ m}^3$ was used. The fluid movement was recorded using Particle Image Velocimetry (PIV) and High Speed Camera.

The sampling in the industrial process was performed during continuous casting of stainless steel.

Separation of droplets - Similarity criterion and dimensional analysis

To scale up the distance L_m of the flow velocity in the vicinity of a fluid - fluid interface measured in the model to the distance of flow velocity in the casting mould L_c , the Weber and Froude similarity criterion and a scale factor as well as the ratio $\varphi = L_m/L_c$ were used^[21]. The dimensionless Froude number, which represents the ratio of momentum to buoyancy force, is given in Eq. (2)

$$Fr = \frac{u^2}{gL} \equiv \frac{F_p}{F_g} \quad (2)$$

where u is the velocity, g is the force of gravity and L is the characteristic length. The Weber number ensures equal ratios of the momentum to interfacial tension force,

$$We = \frac{u^2 L \rho}{\sigma} \equiv \frac{F_p}{F_\sigma} \quad (3)$$

where ρ is the liquid density of the continuous liquid and σ the interfacial energy between continuous and dispersed liquid. Applying φ in Eq. (2) and (3), we derive a scale factor λ of about 0.5 (Eq. 4) using densities and interfacial tension of the model liquids (Index m) and the steel - slag systems (Index s),

$$\lambda = \left(\frac{\rho_s \sigma_m}{\rho_m \sigma_s} \right)^{1/2} \sim 0.5. \quad (4)$$

Thus the measured velocity in the model is equal to a bulk velocity at a distance L_c of 16 mm in steel - slag system. When a fluid interface is exposed to a shear force from a flow initiated by a rotating roller, the meniscus is deformed. The flow acts tangentially on the interface leading to the formation of finger - like protrusions. The interfacial energy acts against the tendency for droplet break-up. In order to describe the flow - induced break-up of droplets dimensionless relations are derived. The flow velocity needed for the entrainment is a function of the material properties of the phases (Eq. 5)^[21].

$$u_{crit.} = f\{\rho_c, \rho_d, \eta_c, \eta_d, \sigma, g\}. \quad (5)$$

Here η_c and η_d are the viscosities of the continuous and disperse phases, $u_{crit.}$ the critical speed in the vicinity of the liquid - liquid interface when droplet break-up starts, σ is the interfacial energy between the two liquids, ρ_c and ρ_d are the densities of the continuous and disperse phases and g is the force of gravity. Applying the Π - Theorem^[22] we achieve the Π - groups listed in Table 1.

Table 1: Π - groups

$\Pi_1 = \sigma/u \eta_c$	$\Pi_2 = u^3 \rho_d / \eta_c g$
$\Pi_3 = u^3 \rho_c / \eta_c g$	$\Pi_4 = \eta_d / \eta_c$

The reciprocal of Π_1 is the ratio of the deforming stress exerted by the continuous phase and the counteracting Laplace pressure and is called the capillary number Ca (Eq. 6)

$$\frac{1}{\Pi_1} = \frac{u \eta_c}{\sigma} = Ca. \quad (6)$$

This dimensionless number represents a stability criterion for a liquid - liquid interface exposed to a shear stress and given properties of liquids. The combination of Π_2 and Π_3 leads to the viscosity ratio ρ_c/ρ_d and Π_4 is the viscosity ratio η_d/η_c . The product of η_d/η_c and ρ_c/ρ_d is a dimensionless number (ν_d/ν_c) describing only material parameters and is called material number Λ . Therefore the relationship between different Π - groups containing the properties and forces acting in the analyzed system are defined as follows:

$$\Pi_1 = f(\Pi_2, \Pi_3, \Pi_4). \quad (7)$$

Inserting the definitions from Table 1:

$$Ca = f\left(\frac{\eta_d}{\eta_c}; \frac{\rho_c}{\rho_d}\right) \quad (8)$$

Defined in this way, increasing value of Λ would correspond to a retardation of the droplet separation. Finally, the relationship between the driving forces and material properties for droplet break-up is defined as following:

$$\frac{u \eta_c}{\sigma} = f\left(\frac{\nu_d}{\nu_c}\right). \quad (9)$$

Here ν_c and ν_d are the kinematic viscosities of the continuous and dispersed phase.

Interfacial convection and mass transport – problem analysis and basic description

For the problem of interest here relates to how local disruption of the interfacial tension affects the flows in a slag layer on top of the liquid metal. The details of this analysis are described in the previous papers ^{[16][19][23]}.

The movement of a briefly accelerated volume element or fluid layer is determined by a given interfacial tension force F_σ (corresponding to $\Delta\sigma$) acting as a result of the disturbance in a local area on the interface, the inertia force F_ρ and the viscous force F_η . As the velocity in metallurgical systems cannot normally be measured in experiments at such short distances (movement at the boundary layer), only the variables describing the acting forces and the characteristic length can be considered for a description of the problem (variables L_c, σ, ρ, η). An analysis of the problem with the aid of the similarity theory gives the following expression to describe fluid movement in the boundary layer area:

$$L_c \Delta\sigma \rho \eta^{-2} \equiv \frac{F_\sigma F_\rho}{F_\eta^2} \quad (10)$$

where $L_c \Delta\sigma \rho \eta^{-2}$ is denoted the Steinmetz number Ste in honour of Professor Eberhard Steinmetz as derived in the

previous papers ^{[19][1]}. An identical expression is obtained by division of the known numbers Re and We , Re^2/We . By linking the acting forces in the form of the above-mentioned value (equation 1), the overall relationship for convection flows is maintained without flow velocity being a factor.

For an identical disruption of the interfacial energy ($\tau_{max} = \Delta\sigma/\Delta x = \text{constant}$) increasing layer thickness will give a constantly strong impulse at an even greater distance from the disruption. When viewed perpendicularly to the phase boundary, layers further away from the interface are also move due to friction and the impulse decreases with the distance from the interface. As stated previously, this gradient is the greater, the thinner the layer. For the respective fluid, however, $\text{grad } \tau$ decreases with increasing Ste (because $Ste \sim L_c$ or Δy) and in parallel greater fluid volume near the interface is moved. It is therefore logical to use the Steinmetz number Ste to characterize the flow conditions in thin fluid layers caused by gradients of interfacial tension.

Mass transport

Three dimension free numbers as Sh , St and Bo , Sherwood, Stanton and Bodenstein respectively, are usually used to describe the mass transport. With respect to the analysis of the mass transport description discussed in the introduction, the Bo -number is suitable for the description of the problem. For improved evaluation of the measured values the modified Bodenstein number Bo^* is new defined, as the mass flow caused by diffusion cannot be separated from mass flow caused by convection in experimental investigations. It defines the quote of the total (measured) mass flow rate density of analysed species which results from the transferred mass through the interface in the reaction time $\dot{m}_{i,\Sigma}$ to the mass flow rate density caused by diffusion $\dot{m}_{i,D}$:

$$Bo^* = \frac{\dot{m}_{i,\Sigma}}{\dot{m}_{i,D}} \quad (11)$$

If the upper fluid (e.g. slag) is assumed as completely still without any convection so the species i will be transported in this fluid only by the diffusion. If the interfacial reaction controls the total rate than is the $Bo^* \leq 1$. Otherwise if the reaction products or transferred species are transported away by convection (e.g. thermal or interfacial convection) than is the $Bo^* > 1$. If interfacial convection occurs they are squeezed from the diffusion layer to the bulk followed by “fresh” liquid. The mass transfer through the interface causes the local change in the interfacial energy which itself generate the movement at or near the interface. Following, the relationship between the interfacial convection and mass transport have been proposed in the previous paper ^[19]:

$$Bo^* = \text{const. } Ste^z \quad (12)$$

2.2. Material used

With the knowledge of Λ for the steel - slag system the model - liquids for the cold model study of droplet separation were chosen. *Table 2* shows the properties of the Newtonian liquid used (density ρ , dynamic viscosity η and interfacial energy σ). Water was used as continuous phase for all experiments. Silicon oils are used to develop a liquid -liquid interface with differing viscosity ratios. The silicon oils behave like Newtonian liquids, i.e. their viscosity is unaffected by shear (for η 0.6 - 970 mPas).

Table 2: Properties of the liquids used for model investigations at 298 K

Liquid	Phase	Density	Viscosity	Interfacial tension against H ₂ O	Λ
		[kg m ⁻³]	[kg m ⁻¹ s ⁻¹]	[N m ⁻¹]	
Silicon oilAk0.65	disperse	760	0.0006	0.040	1
Silicon oilAk5	disperse	920	0.0046	0.040	5
Silicon oilAk10	disperse	930	0.0093	0.040	10
Silicon oilAk35	disperse	955	0.0330	0.041	34
Silicon oilAk50	disperse	960	0.0480	0.041	50
Silicon oilAk100	disperse	963	0.0960	0.042	99
Silicon oilAk200	disperse	966	0.1930	0.044	199
Silicon oilAk500	disperse	969	0.4850	0.044	499
Water	continuous	997	0.0009	-	-

In the investigations of interfacial flow, different non-miscible fluids were layered above one another. Deionised water was always covered by different fluids with lower densities. The adjustable parameter was the height of the covered layer which was varied within the range of 3 mm to 12 mm, see *Table 3*. Depending on the properties and the height of the upper layer as variable parameter, the dimensionless Steinmetz number *Ste* (eq. 10) can be calculated. The numerical values of *Ste* for the variation of the fluid combination and the varied ranges of the upper layer are given in *Table 3*.

Table 3 Calculated Steinmetz number for different upper layer height and substances overlaying water

Thickness of the upper layer [mm]	Steinmetz number (<i>Ste</i>)		
	Oil	Hexanol	Petroleum
3	7	172	34·10 ³
5	12	287	57·10 ³
6	14	344	68·10 ³
10	23	573	114·10 ³
12	28	688	137·10 ³
20	47	1146	228·10 ³

A high speed camera was used to record the movement of a dyed tracer at the interface between the two non-miscible fluids from a top view. Furthermore, the particle image velocimetry (PIV) with Rhodamin B particles of about 20 μm diameter were used as tracer in both phases. For the observation and measurement of the mass transport the similar experimental arrangement as described above was used. As immiscible liquids butanol and water were used and the transfer of Rhodamine 6G as tracer substance from water to butanol was measured using the laser induced fluorescence (LIV) method after the same laser was calibrated for the new system. In one case the transport of Rhodamine 6G only by diffusion was measured while in other case its change due to induced interface convection. The details are described in the previous paper ^[16].

In the industrial experiments samples were taken from the mould during the continuous casting process. Mass exchange between mould flux and stainless steels with different Ti content were measured by analysing of quenched

mould flux. The chemical composition of steels and mould fluxes are given in previous paper [24].

3. Results and discussion

Droplet separation in non reacting fluids

Figures 4a) to d) show a sequence for entrainment of silicon oil Ak50 - water system. With increasing roller-speed, a meniscus with finger - like protrusion is formed. When a critical rotation speed is reached, droplet break-up takes place, d). During this process the formation of satellite droplets is observed. Up to a viscosity ratio of $\nu_d/\nu_c > 50$, the length of the finger-like protrusion and thus, the possibility of disintegration into more than one droplet are found to increase.

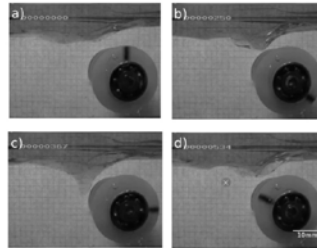


Figure 3 Sequence for meniscus formation and droplet break-up for system silicon oil Ak50 (upper phase) and water (white cross marking entrained droplet).

Theoretical and experimental studies of Rallison and Strove [7][25] point out that the break-up of Newtonian liquid droplets entrained in an immiscible liquid depends only on Ca and η_d/η_c if inertial effects are negligible. In steel - slag systems, the density differences are significant and therefore, the impact of the same has to be taken into account. For the model liquids used in our experimental study ρ_c/ρ_d was varied from 1.0 to 1.3. The critical values of Ca - and Λ - number for the start of droplet separation at each liquid combination and flow velocity at the distance of 8 mm from the liquid - liquid interface is plotted in Figure 4. For each fluid combination and therefore fixed Λ -value, three measurements on break-up were made.

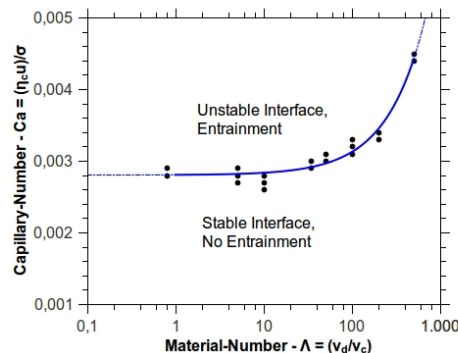


Figure 4 Dimensionless relation between the capillary and material number for the start of droplet break-up at fluid interface.

The critical values for Ca and Λ , at which the droplet separation starts, divide the parameter area in a stable interface with no entrainment (Ca -values below Ca^*) and the area of a unstable interface with entrainment of the upper

liquid (Ca - values higher than Ca^*). For the range $0.001 < \Lambda < 10$, the capillary number is constant. In this region, the Ca^* is independent of Λ and the droplet separation from upper fluid can be prevented by keeping the value of Ca lower than Ca^* . For $\Lambda > 10$, the critical capillary number increases. Beyond $\Lambda=500$, we assume a drastic increase of Ca^* as reported by Strove^[25] for high viscosity ratios in a cone - plate device. In order to ensure the stability of a liquid - liquid interface e.g. the slag viscosity can be increased resulting in higher values of Λ . On the other hand the increase of interfacial energy σ results in lower values of system capillary number as well as the reduction of the flow velocity u near the interface.

Using the material properties and measured interfacial energy σ ^[26] and assuming a metal flow of 0.3 m/s^{[27][28]} in the vicinity of the steel - slag interface in the industrial mould, the values of Ca can be calculated. For the investigated steel - slag systems^[26] the Ca - numbers are in the range $1.55 - 2.73 \times 10^{-3}$ and are significantly lower compared to the critical values obtained in experimental model investigation (compare Figure 6). Assuming the conditions mentioned above the steel - slag interface should be stable and droplet break-up should not appear. However extremely small slag inclusions are frequently found in rolled materials which indicate that in the casting process dispersion or emulsification processes occurs. The reason for this is the effect of interfacial energy and interfacial convection and probably local decrease of slag viscosity. These phenomena are the subject of the following chapter.

Mass transport and mass exchange near the interface

The propagation velocity at the interface observed in cold model with high speed camera is given by the measured displacement of the dyed tracer. The measured velocities are plotted over the distance from the surfactant injection position (disruption position) as shown in Figure 5. The results show that with increasing layer thickness the movement velocity increases for constant material properties. Assuming that the total reduction of the interfacial tension $\Delta\sigma$ corresponds with the interfacial tension σ between the both phases the Steinmetz number can be calculated.

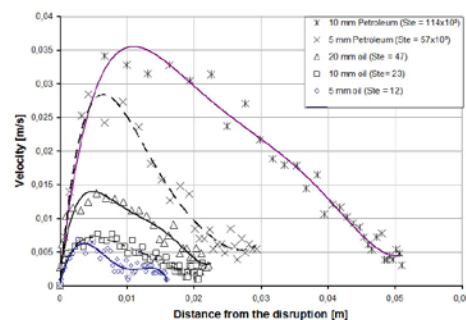


Figure 5 Dependency between the velocity of the tracer and distance from the injection position [16].

The velocity of the area nearest to the injection position, in which interface undergoes an acceleration from a static position, increases with liquid layer thickness and following the growing Steinmetz number. After reaching a maximum, it decreases with increasing distance from the injection position. It can be deduced that the spatial magnitude of the velocity depends on Steinmetz number. The maximal velocities for the point in certain distance of the point of disruption are depicted over the varied Steinmetz number, as shown in Figure 6. For more accurate observation using the high speed camera a good correlation between the Ste number and the velocity near the interface is observed. In the

continuous casting processes liquid fluxes are in contact with liquid steel. For this case with flux layer thickness above the meniscus of $L_c = 5$ mm and assuming change of σ down to zero the Ste values is $2.7 \cdot 10^3$ to $5.4 \cdot 10^3$. Therefore the range of the Ste values of liquid used in present experiments covers also the metallurgical conditions.

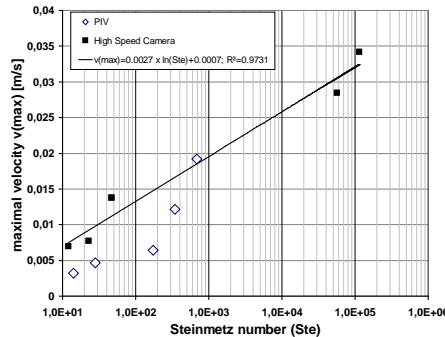


Figure 6 The maximal velocity at the interface as a function of Ste number measured with PIV method and high speed camera.

The effect of sudden and local change of interfacial energy on interfacial convection was measured using the LIF method. The two dimensional area was enlighten by YAG-laser and the fluorescence intensity as a measure for the concentration was recorded with CCD camera (FlowSense M2 8bit). After the injection of surfactants the torus vortex on both sides of the interface are generated which support the turbulent mass transport near the interface and increase finally the mass exchange between the phases. The situation showing the local turbulence near the interface is given in Figure 7.

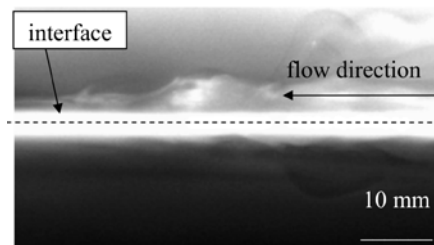


Figure 7 Turbulence near the interface caused by surfactant addition recorded using LIF method.

In the casting process considered here, the sources of oxygen are (FeO) and (SiO₂), with [Ti], [Mn] and [Cr] being oxidised (parentheses and square brackets denote slag phase and metal phase respectively). The greatest exchange, in particular with Ti alloyed steel grades, takes place between (SiO₂) and [Ti]. Since [Ti] was present in different concentrations in the alloys examined, and the change in the (TiO₂) concentration was the highest of all components, the effect of the convective flows on the kinetics of the metal-slag reaction was examined on the basis of [Ti] oxidation and absorption into the slag. The effect of interfacial convective flows on the kinetics of the mass transfer with liquid metal was investigated via the ratio $\Delta(\text{TiO}_2) / [\text{Ti}]$ (where Δ represents the difference in the chemical composition of sampled slag and the original powder) as a function of the slag layer thickness^{[11][23]}. The ratio increases with slag layer thickness of 5-6 mm.

The relationship between the Bo^* and the convection conditions in the slag, as defined by the Steinmetz number Ste ,

are examined below. To analyse the problem, a combination of the metal alloy and the slag is considered in each case. This ensures that the mass transfer (and thus the mass transfer coefficient) for each system considered can be assumed to be constant. Therefore, the modified Bodenstein number Bo^* , defined in equation (2), takes into consideration the effect of the convection conditions for each slag-metal combination in the same way.

The experimental results evaluated in this way are shown in Figure 8. It can be clearly seen that Bo^* increases with increasing Ste . Even with the smallest measured slag layer thickness, Bo^* is greater than 1 (i.e. the total mass transport is greater than the diffusive mass transport). It can be reliably assumed that under the experimental conditions, the interfacial flows always occur as soon as liquid slag is formed. They make a basic contribution to the total mass transport up to approx. 20 times the mass flux by diffusion (see values of Bo^* in Figure 8).

The values of the Ste number are between $2 \cdot 10^3$ and $5 \cdot 10^3$ and lies within the range of experiments performed at room temperature. Following it can be derived that flow conditions near the interface in the real metallurgical process can be described using the Ste number.

For values of Ste higher than ca. $5 \cdot 10^3$ (marked with thick stroke), thermal convection occurs and the relation between Bo^* and convective flows has to be described using another function as reported previously [11][19]. In this case the flow conditions are described by the product $Ste \cdot Ra$, which takes into account as well the interfacial convection as the thermal one.

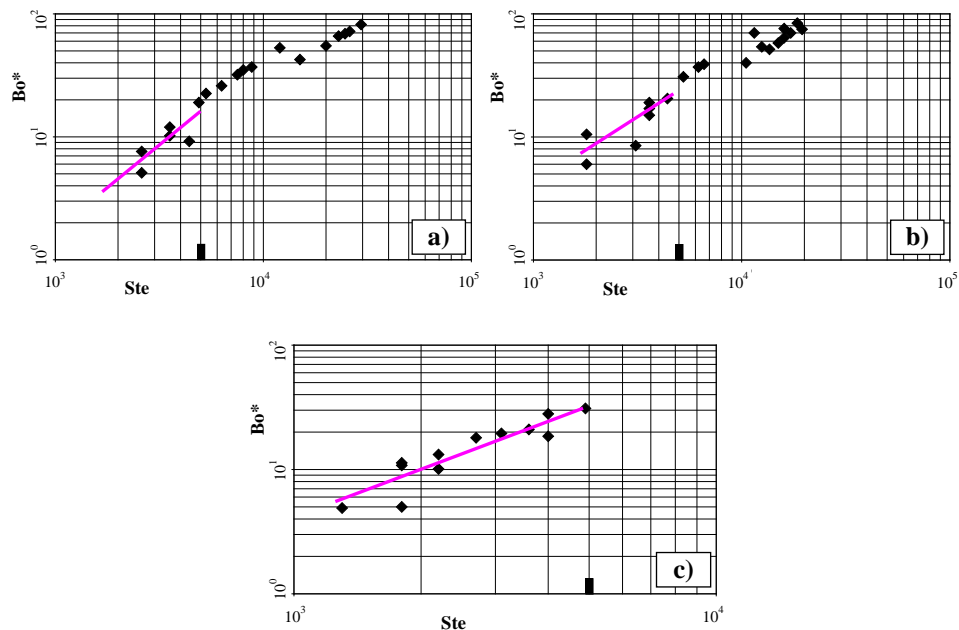


Figure 8 Modified Bodenstein-number Bo^* for TiO_2 -absorption into the casting flux as a function of Steinmetz-number Ste (valid in the range of Ste up to $5 \cdot 10^3$) for cast steel grades a) AISI 304 b) AISI 321 and 316Ti c) AISI 409 and 430Ti

In the carefully arranged experiments in the CLSM the surface of liquid metal and the slag boundary on the liquid metal were observed. After few minutes of observation the samples were quenched and then investigated by optical

microscopy after the metallographic preparation. Near the surface or interface (in the distance less than approx. 200 μm) slag droplets with diameter up to approx. 15 μm were detected, Figure 9a) [29]. Using SEM-EDX it was revealed that the entrained droplets had the same composition as the slag used. A similar nature of slag entrapment was found in the experimental works of Chung and Cramb [30][31]. In the industrial trials samples were taken in the mould during the casting process. Also in these samples mould slag droplets of similar size and distance from the slag-metal interface were found, Figure 9b) [1].

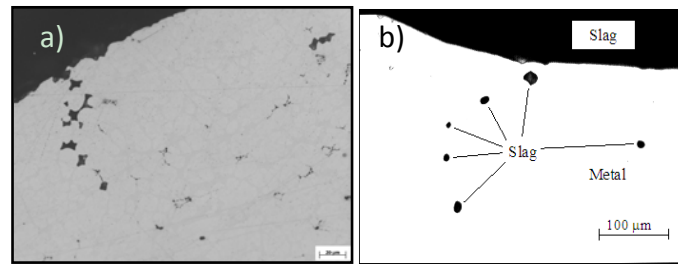


Figure 9 Interface between CrNi-steel and slag, a) $\text{CaO-SiO}_2\text{-TiO}_2$ slag (dark) , b) mould slag.

For the analysis of the emulsification process of slag in liquid metal the dimension free numbers, Ca and A as described above, were analysed. The macroscopic emulsification observed occurs, if the values of Ca and A lie above the stability line and no emulsification takes place, if they lie below this line in the Figure 4 [26]. For fixed material properties described by A and fluid flow velocity the emulsification will occur, when the interfacial energy (in the denominator of Ca) decreases to low enough values. For the liquid metal flow velocity of 0.3 to 0.4 ms^{-1} , which exists near the slag/metal interface e.g. in the continuous casting process, the microscopic emulsification can take place if the interfacial tension diminishes below approx. 100 mNm^{-1} . Such values are possible as reported in the previous papers [24][32]. In this case the force acting parallel to the interface accelerate the liquids on both sides of the interface. Due to the difference of the viscosities of both liquids the Kelvin-Helmholtz interfacial instability occurs at the interface which leads to the emulsification of slag in metal and also of metal in slag.

4. Conclusions

The separation of droplets at the interface of two non reacting and immiscible liquids was investigated in the physical cold model and criteria for the separation are derived.

Flow conditions in thin overlaying liquid layer caused by the disturbance of interfacial energy between two immiscible liquids have been described theoretically and the results of laboratory experiments are presented. A dimension free number $L_c \Delta \sigma \rho \eta^{-2}$ or Ste (Steinmetz number), describing convective flows next to the interface in the liquid boundary layer caused by the disturbance of interfacial energy have been experimentally tested for different combination of fluids. Flow induced by interfacial energy disruption has been investigated experimentally using a high speed camera and particle image velocimetry (PIV). The effect of interfacial flow on mass transport near the interface was recorded using laser induced fluorescence (LIF) and described by modified Bodenstein number Bo^* . The results can be summarized as follows:

- i) The dimension free numbers containing the physical properties of liquids being in contact and the flow velocity near the interface, $Ca = u \eta_c / \sigma$ and $A = v_d / v_c$, are derived. They are suitable for the description of conditions, at which the droplet separation occurs or can be avoided. The consequences for slag droplet separation at the continuous casting conditions are discussed.
- ii) An abrupt local decrease of interfacial tension induces toroidal vortices in the thin liquid layer with free surface. In the lower liquid layer a similar recirculation movement of liquid was observed.
- iii) The movement velocity of the volume elements near the interface increases with increasing values of Ste as well as the moved liquid volume.
- iv) The dimensionless Ste number is suitable for the description of convective flows caused by the disturbance of interfacial tension.
- v) The modified Bodenstein number Bo^* describing the quote of mass transport rate density caused by diffusion and convection related to the one caused only by diffusion is suitable for the description of experimental results
- vi) Interfacial convection always occurs at the slag/steel interface regardless of the thickness of the liquid slag layer and the occurrence of free convection. It contributes to the total mass transport up to approx. 20 times the mass flux by diffusion under continuous casting conditions.
- vii) The emulsification of slag as droplets with the diameter smaller then approx. 15 μm into liquid metal can take place under usual process conditions if the interfacial energy decrease to zero or very low values caused e.g. by exchange reactions between both phases.

Acknowledgement

The author like to thank Dr. B. Sahebkar, Ms. R. Drewes and Mr. R. Vardiny for their contribution to this work. The industrial trials and sampling were performed at KruppThyssen Nirosta GmbH which is hereby gratefully acknowledged. The research was partially supported by the DFG (German Research Foundation) under project No. 051201019. This is gratefully acknowledged.

List of symbols

A	reaction area	g	force of gravity
Bo	Bodenstein number	L_c	characteristic length
Bo^*	modified Bodenstein number	L_m / L_c	characteristic length in the model/ continuous casting mould
C	concentration		
Ca	capillary number	L_s	slag layer thickness
D	diffusion coefficient	\dot{m}	mass flux density
d	droplet diameter	n	rotation rate
F_η	viscous force	Ra	Rayleigh-number
F_ρ	inertia force	Re	Reynold-number
F_σ	surface tension force	Sh	Sherwood-number
Fr	Froude number	Ste	Steimetz-number

T	absolute temperature	[]	metal phase
u	fluid velocity	()	slag phase
v	velocity		
We	Weber-number	<i>Indices</i>	
A	material properties number	c	continuous phase
λ	scale factor	d	dispersed phase
η	dynamic viscosity	D	diffusion
ν	kinematic viscosity	M	metal
Π	variable of dimensionless group	S	slag
ρ	density	Σ	total
σ	interfacial tension	i	substance i
τ	shear stress		

References

- [1] P.R. Scheller: High Temp. Materials and Processes 22 (2003) 5-6, 387
- [2] J. Park: Materials Science and Engineering A, 2008, vol.472, pp. 43-51.
- [3] B.G. Thomas: Proceedings of the 35th Meeting of the International Continence Society, 2005, Montreal, Canada.
- [4] J. Savolainen, T. Fabritius and O. Mattila: ISIJ International, 2009, vol.49, pp. 26-36.
- [5] J. Harman and A. Cramb: Steelmaking Conference Proceedings, 1996, pp. 773-783.
- [6] J. Janssen, A. Boon and W. Agterof: AIChE Journal, 1994, vol.40, pp. 1929-1939.
- [7] J. Rallison: Annu. Rev. Fluid Mech., 1984, vol.16, pp. 45-66.
- [8] B. Gelfand: Pro. Energy Combustion Sci., 1996, vol.22, pp. 202-263.
- [9] H. Stone: Annu. Rev. Fluid Mech., 1994, vol.26, pp. 65-102.
- [10] E. Steinmetz: Arch. Eisenhüttenwes. 43 (1972), 151
- [11] P.R. Scheller: 3rd European Conf. Cont. Casting Proc., Madrid, Spain, Oct. 20-23, 1998, 797
- [12] T. Takasu; J.M.Toguri: Philosophical Trans. Royal Soc. A: Mathematical, Physical and Engineering Sciences 356 (1998) No 1739, 967
- [13] M.A. Rhamdhani; K.S. Coley; G.A. Brooks: Proc. 43rd Annual Conf. of Metallurgists of CIM 2004, Hamilton, CA, 203
- [14] M.A. Rhamdhani; K.S. Coley; G.A. Brooks: Met. Mat. Trans. B 36B (2005) 5, 591
- [15] C.V. Sterling; L.E. Scriven: AICHE J. 5 (1959), 514
- [16] P.R. Scheller: Proc. SANO Symposium, University of Tokyo, pp 84-95, Tokyo Oct. 1-3, 2008
- [17] P.R. Scheller: Habilitation Thesis: Flow conditions and mass exchange in thin liquid layer with special view to continuous casting fluxes, Aachen University RWTH, May 1998
- [18] Y. Chung; A. Cramb: Met. Mat. Trans. B 31B (2000) 10, 957
- [19] P.R. Scheller: Ironmaking & Steelmaking 29 (2002) 2,154
- [20] Avidemux 2.5.2 documentation <http://www.avidemux.org>

- [21] L. Zhang, S. Yang, K. Cai, J. Li, X. Wan and B.G. Thomas: Metallurgical and Materials Transactions B, 2007, vol.38, pp. 63-83.
- [22] P. Grassmann: Physikalische Grundlagen der Verfahrenstechnik, 1983, 3.Auflage, Verlag Sauerländer AG, Aarau.
- [23] P.R. Scheller: steel research int., 76 (2005), 581
- [24] P.R. Scheller: steel research int., 81 (2010) 10, 886
- [25] P. Strove and P. Varanasi: Journal of Colloid and Interface Science, 1984, vol.99, pp. 360-373.
- [26] R. Hagemann and P.R. Scheller: Submitted to Metallurgical and Materials Transactions B 2011.
- [27] M. Assar, P. Dauby, and G. Lawson: Proceedings of the 83th Steelmaking Conference, 2000, Pittsburgh, USA.
- [28] P. Dauby: Proceedings of the Roderick Guthrie Honorary Symposium on Process Metallurgy, 2011, Montreal, Canada.
- [29] R. Hagemann; P.R. Scheller: CAMP-ISIJ Vol. 24(2011)-509.
- [30] Y. Chung and A. Chramb: Metallurgical and Materials Transactions B, 2000, vol.31, pp. 957-971.
- [31] Y. Chung; A. Cramb: Phil. Trans. R. Soc. London A, 1998, vol. 356, 981.
- [32] P.R. Scheller: VII Int. Conf. On Molten Slags, Fluxes & Salts, 25-28 January 2004, Cape Town, South Africa, p.411.